QCD in background magnetic fields – an overview of recent lattice results

Gergely Endrődi[*]

Institute for Theoretical Physics, Universität Regensburg, D-93040 Regensburg, Germany.
E-mail: gergely.endrodi@physik.uni-regensburg.de

In this talk I give an overview of recent developments in the field of lattice QCD with background magnetic fields. A special emphasis is put on the discussion of methods to determine the equation of state and the magnetic susceptibility of the thermal QCD medium. The results are compared to the hadron resonance gas model at low and to perturbation theory at high temperatures. In addition, possible implications of the QCD magnetic response for heavy-ion collisions are addressed.

---

[*]Speaker.

http://pos.sissa.it/
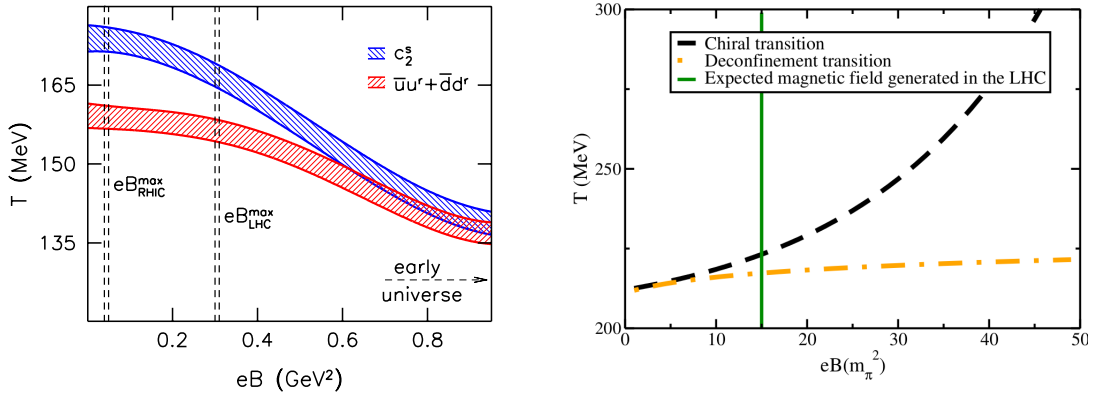
1. Introduction

Background (electro)magnetic fields represent an important concept for the description of various aspects of high-energy particle physics. Besides their role in dense neutron stars (magnetars) and in cosmological models of the early universe, background magnetic fields have a characteristic influence on the early stages of non-central heavy-ion collisions, see, e.g., the recent review [1]. In addition to the phenomenological relevance of the magnetic field, it also represents a new direction to probe the strong interactions, and – besides the temperature and the density – may be thought of as a third axis in the phase diagram of Quantum Chromodynamics (QCD). The magnetic field B turns out to be a very effective probe, since it separates the electrically neutral gluonic and the electrically charged quark degrees of freedom, enabling a deeper understanding of the complex QCD dynamics.

From the technical point of view, a feature of background magnetic fields making them particularly attractive is that the corresponding lattice formulation is free of the sign problem. Thus, QCD in the presence of magnetic fields is amenable to standard Monte-Carlo methods based on importance sampling. This allows for a fully non-perturbative determination of, for example, the phase diagram of the theory in the magnetic field-temperature plane. This phase diagram has been calculated in Ref. [2] using the staggered quark discretization with physical masses and is shown in the left panel of Fig. 1 (for further lattice results on the phase diagram, also with different discretizations, see Ref. [3]). One of the most striking features of this plot is that it reveals just the opposite of what most low-energy effective models of QCD have predicted. Instead of having an increasing transition temperature $T_c(B)$ found in, for example, the linear sigma model [4] (see the right panel of Fig. 1), the transition temperature monotonously *decreases* in the region $0 < eB < 1$ GeV^2. The most important ingredient to this behavior is the dependence of the quark condensate and the Polyakov loop on B [5]. The inconsistency of the model prediction with the lattice results has stimulated a range of new studies and made the phase diagram with magnetic fields the subject of lively discussions. For details the reader is referred to the recent review [6].

Figure 1: Left panel: the QCD phase diagram in the temperature-background magnetic field plane, using continuum extrapolated lattice results [2]. The red band represents the inflection point of the average light quark condensate, while the blue band that of the strange quark number susceptibility. Right panel: the QCD phase diagram predicted by the linear sigma model [4].

In fact, QCD at $B > 0$ – and in particular, the question whether $T_c(B)$ increases or decreases –

has become an effective testing ground for low-energy models, functional approaches and effective theories. In the present talk I will argue that besides the phase diagram, the equation of state (EoS) may also provide a non-trivial check of low-energy models. The EoS describes the fundamental relation between thermodynamic observables like the pressure, the energy density etc., and thus encodes the thermodynamic properties of the system. As recent lattice simulations have shown, the EoS also exhibits a complex dependence on the magnetic field, arising from the transition between the low-energy hadronic regime and the high-temperature quark-gluon-plasma. In addition, there are also various aspects of the EoS at $B > 0$ that might have implications for heavy-ion collision phenomenology and that will be addressed briefly during the talk. For recent talks on this subject, see Ref. [7], and for recent reviews on the lattice results, Ref. [8].

2. Magnetic susceptibility and free-case prediction

Let me start the discussion about the $B > 0$ EoS with a general remark. Based on the linear response to background magnetic fields, materials can be classified into two categories: paramagnets and diamagnets (excluding ferromagnets, where the response is non-linear). Thermal QCD matter can also be considered as a medium that can be characterized in this respect. More precisely, this response is encoded in the B-dependence of the free energy density

$$f(B) = -\frac{T}{V} \log \mathcal{Z}(B), \tag{2.1}$$

given in terms of the partition function $\mathcal{Z}$ of the system, the temperature T and the spatial volume V. The leading response is given by derivatives of the free energy density,

$$\mathcal{M} = -\frac{\partial f}{\partial (eB)}, \qquad \chi = -\frac{\partial^2 f}{\partial (eB)^2}\bigg|_{B=0}, \qquad \chi_r = \chi - \chi|_{T=0} \tag{2.2}$$

where the magnetic field is considered in units of the elementary charge $e > 0$ for later convenience. The magnetization $\mathcal{M}$ vanishes at $B = 0$ due to parity symmetry. The first non-trivial expansion coefficient is the magnetic susceptibility χ. As will be explained below, in a quantum theory it undergoes additive renormalization and its renormalization amounts to subtracting its value at $T = 0$. After this renormalization is performed, the sign of χ_r can be used to distinguish between paramagnetism ($\chi_r > 0$) and diamagnetism ($\chi_r < 0$).

It is instructive to first calculate the susceptibility for electrically charged but otherwise non-interacting particles. In this setup – which will be referred to as the free case in the following – the $T = 0$ free energy can be determined analytically using Schwinger's proper time formulation. Subtracting the $B = 0$ contribution, $\Delta f = f(B) - f(0)$, and expanding in B one finds that the quadratic term is logarithmically divergent in the cutoff Λ and equals $\beta_1 (qB)^2 \log \Lambda/m$. Higher-order terms are, on the other hand, ultraviolet finite. The logarithmic divergence is canceled through a renormalization of the energy $B^2/2$ of the magnetic field [9],

$$\frac{B^2}{2} = \frac{B_r^2}{2} - \beta_1 (qB)^2 \log(\Lambda/\mu), \tag{2.3}$$

where μ is a renormalization scale and β_1 is the lowest-order QED β-function coefficient. In the fermionic and bosonic cases, it reads

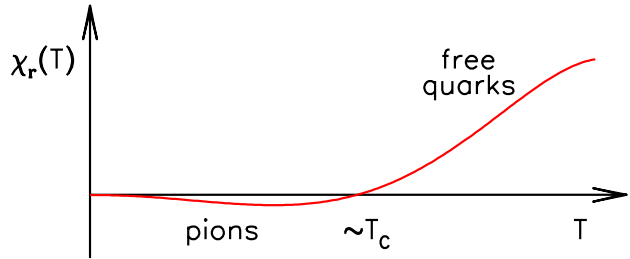$$\beta_1^{\mathrm{f}} = 1/(12\pi^2), \qquad \beta_1^{\mathrm{b}} = 1/(48\pi^2). \tag{2.4}$$

Note that higher-order QED corrections to the β-function are absent since the magnetic field is external [9, 10]. The purely magnetic contribution $B_r^2/2$ is independent of the medium and is therefore excluded in the following. In the on-shell renormalization scale $\mu = m$ one finds that the wave-function renormalization (2.3) exactly cancels the $\mathcal{O}(B^2)$ contribution in the free energy density and the resulting renormalized free energy is of $\mathcal{O}(B^4)$. Thus, differentiating with respect to B the susceptibility (2.2) vanishes. At $T > 0$ thermal effects induce a finite contribution to Δf to quadratic order and, thus, a non-vanishing value of the susceptibility.

Employing the proper-time representation for $T > 0$, the susceptibility is found for bosons and for fermions, respectively [10],

$$
\begin{aligned}
\chi_r^{\mathrm{f}}(T) &= -\beta_1^{\mathrm{f}} \int_0^\infty \frac{\mathrm{d}s}{s} e^{-m^2 s} \left[\Theta_3\left(\frac{\pi}{2}, e^{-1/(4sT^2)}\right) - 1 \right] \xrightarrow{T\to\infty} 2\beta_1^{\mathrm{f}} \log T/m, \\
\chi_r^{\mathrm{b}}(T) &= -\beta_1^{\mathrm{b}} \int_0^\infty \frac{\mathrm{d}s}{s} e^{-m^2 s} \left[\Theta_3\left(0, e^{-1/(4sT^2)}\right) - 1 \right].
\end{aligned}
\tag{2.5}
$$

Here, m is the mass and q the electric charge of the particle and Θ_3 is an elliptic Θ-function resulting from the sum over Matsubara-frequencies. The crucial difference between bosons and fermions is the temperature-dependence given by the square brackets in Eq. (2.5), being negative for fermions and positive for bosons. Given the positivity of the β-function coefficients (2.4) – neither spinor nor scalar QED are asymptotically free – one sees that bosons are always diamagnetic, whereas fermions paramagnetic. From the classical point of view, this may be understood from the fact that bosons couple to B only via their angular momentum, and this magnetic moment always works against the magnetic field due to Lenz's law. Fermions, however, also interact with B through their spin and this magnetic moment overweighs the one due to angular momentum. In particular, for high temperatures, the fermionic susceptibility rises logarithmically with T, as indicated in Eq. (2.5).

Employing these findings, we can predict the dependence of the QCD magnetic susceptibility on the temperature, see Fig. 2. At $T = 0$ the susceptibility vanishes due to the renormalization prescription. At low temperatures, the most important charged degrees of freedom are (quasi-free) pions, which are diamagnetic as we have seen above. At high temperatures, QCD asymptotic freedom dictates that the relevant charged particles are (quasi-free) quarks, which are paramagnetic. The simplest way to connect these three pieces of information is to have a diamagnetic and a paramagnetic region separated by a turning point where $\chi_r = 0$. Since this point is characterized by an effective change of the relevant degrees of freedom from pions to quarks, it is reasonable to expect that it occurs around the transition temperature T_c. Notice that the interplay between the presence of asymptotic freedom in QCD and its absence in QED has played an important role in obtaining the above prediction. Below I will discuss non-perturbative lattice simulations and compare them to this prediction.

Figure 2: Expectation for the QCD magnetic susceptibility based on free-case arguments.

4

3. Magnetic susceptibility on the lattice

As opposed to the case of nonzero baryon chemical potentials, QCD with background magnetic fields can be simulated directly on the lattice. However, calculating Taylor-expansion coefficients like the susceptibility (2.2) turns out to be more complicated for magnetic fields as for chemical potentials. In fact, due to the periodic boundary conditions, the flux of the magnetic field traversing the finite lattice is quantized [11]

$$\Phi \equiv L_x L_y \cdot eB = 6\pi N_b, \qquad N_b \in \mathbb{Z}, \tag{3.1}$$

where we assumed that B is oriented in the z-direction and took into account that the smallest charge in the system (that of the down quark) is $q_d = -e/3$. The surface area of the lattice in the perpendicular direction equals $L_x L_y$. Due to the quantization condition, differentiation with respect to eB is ill-defined and therefore the susceptibility (2.2) is not accessible directly. Recently, several methods were developed to circumvent this problem. They are summarized briefly below.

Anisotropy method   The magnetic field breaks the (Euclidean) Lorentz symmetry of the system. Therefore, the directions parallel and perpendicular to B are distinguished and, in principle, the spatial components of the pressure may become different. A given component of the pressure is defined by the change of the free energy upon an infinitesimal compression of the system in that direction. It turns out that in order to define the perpendicular components $p_\perp$, one must specify what happens to the magnetic field during the compression. Two possibilities are, for example, to keep the magnetic field constant (B-scheme) or, to keep the magnetic flux constant (Φ-scheme) [12]. In the B-scheme, compressing the system in the perpendicular directions decreases the flux, whereas in the Φ scheme, the same compression increases the magnetic field. Clearly, the two schemes describe different physics and give different results for $p_\perp$. While in the B-scheme the pressures are isotropic, in the Φ-scheme [12, 13]

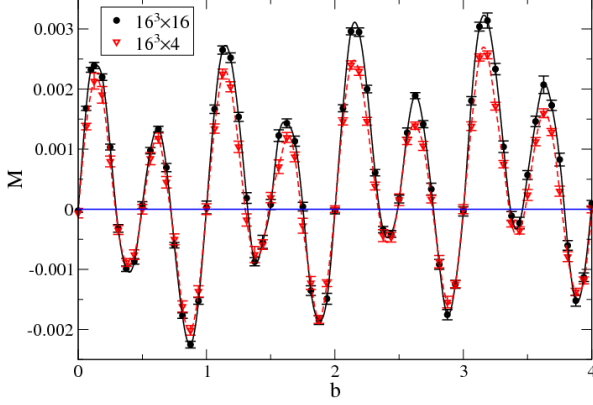$$\Phi\text{-scheme}: \qquad p_\parallel - p_\perp = \mathcal{M} \cdot eB. \tag{3.2}$$

Due to the quantization (3.1) of the magnetic flux, the lattice setup automatically corresponds to the Φ-scheme, and using Eq. (3.2) one can express the magnetization as the difference between the parallel and perpendicular lattice pressures. These can be measured as derivatives of $\log \mathcal{Z}$ with respect to anisotropy parameters. This approach was developed in Ref. [12] and applied at $T = 0$ [12] and later at $T > 0$ [14]. The advantage of the method is that $\mathcal{M}$ is directly obtained as an expectation value for any B, while its drawback is that anisotropy renormalization coefficients also need to be determined.

Half-half method   Instead of the uniform (and, thus, quantized) magnetic field, one can work with an inhomogeneous field which has zero flux, e.g. one that is positive in one half and negative in the other half of the lattice. Since the field strength is now a continuous variable, derivatives of f with respect to eB are well defined and can be measured on a $B = 0$ lattice ensemble [15]. The second-order derivative directly gives the magnetic susceptibility. However, higher-order terms become increasingly noisy, which limits the applicability of the approach to low fields. Note moreover that the discontinuities in the magnetic field enhance finite volume effects. However, it appears that these cancel to a large extent in the renormalized observable $\chi - \chi|_{T=0}$. This method has also been applied to QCD at nonzero isospin chemical potentials and low temperatures in Ref. [16].

Finite difference method For homogeneous magnetic fields, the derivative of f with respect to eB is an unphysical quantity due to the quantization condition, Eq. (3.1). Still, this derivative can be measured for any real value of N_b, and its integral over N_b between two integer values gives the change in f between these two fluxes. In this way, the change of free energies between two integer flux values is constructed as

Figure 3: Reconstructing the B-dependence of the free energy via the finite difference method [17].

$$f(N_{b2}) - f(N_{b1}) = \int_{N_{b1}}^{N_{b2}} dN_b \frac{\partial f}{\partial N_b}. \quad (3.3)$$

Note that while the integral gives the free energy, the integrand $\partial f/\partial N_b$ is not the magnetization but merely an unphysical quantity. It is shown in Fig. 3, revealing a strong oscillation that needs to be kept under control with sufficiently many independent simulations to reliably connect one integer flux with the next. This method was developed in Ref. [17], where it was first employed to determine the $T > 0$ susceptibility for heavier-than-physical quark masses. Later it was applied to QCD with physical quark masses in Ref. [18].
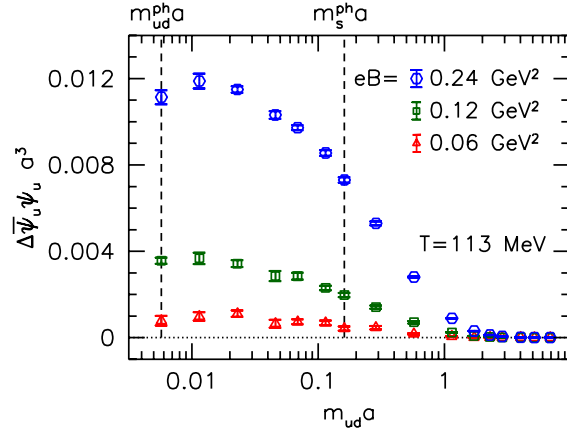
Generalized integral method Finally, the last method, developed in Refs. [10, 13], is based on two observations: that magnetic fields have no effect in pure gauge theory, and that the infinite quark mass limit of QCD (at a fixed magnetic field $qB \ll m^2$) is pure gauge theory. Based on this, the change Δf in the free energy density due to the magnetic field can be expressed as

$$\underbrace{\Delta f(m = \infty)}_{0} - \Delta f(m = m^{\text{phys}}) = \int_{m^{\text{phys}}}^{\infty} dm \frac{\partial \Delta f}{\partial m}, \qquad \Delta \bar{\psi}\psi = -\frac{\partial \Delta f}{\partial m}. \quad (3.4)$$

Thus, Δf at the physical point is obtained via an integral of the quark condensate differences $\Delta \bar{\psi}\psi$ over the quark masses, including unphysically heavy quarks. On a finite lattice, this integral is well regulated and can be calculated in a controlled manner by using 10-20 independent simulations for any given value of the magnetic field, see Fig. 4. Most of these simulations are at large quark masses, where the computation is significantly cheaper. Furthermore, the method automatically gives information on the mass-dependence of f as well.

Figure 4: Reconstructing the B-dependence of the free energy via the generalized integral method [10, 13].
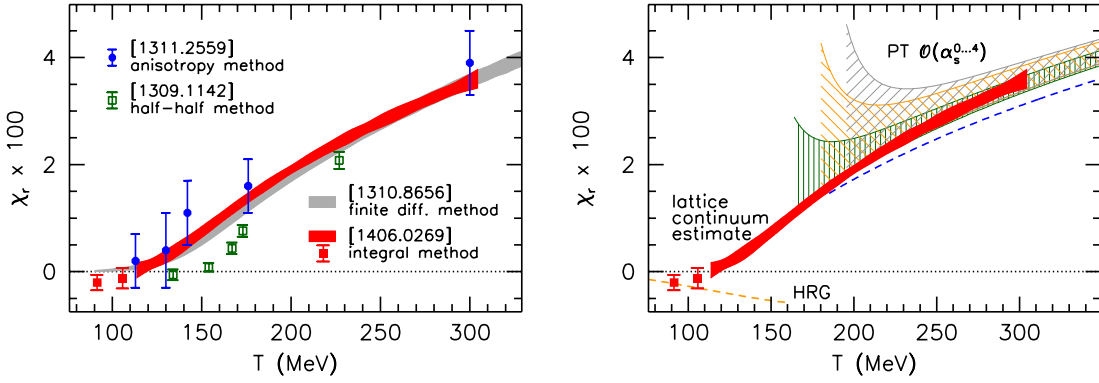
In the left panel of Fig. 5, the susceptibilities obtained using all four methods are summarized. Note that the results employing the anisotropy method [14], the finite difference method [18] and

the generalized integral method [10] are based on the same lattice disretization, using the tree-level improved Symanzik gauge action and stout smeared rooted staggered quarks with physical masses [19]. Perfect agreement within these three approaches is observed. The fourth set of results using the half-half method [15] slightly differs from the other three around T_c, which is attributed to the different action used in that study (somewhat heavier-than-physical HISQ quarks).

The results are in qualitative agreement with the free-case prediction of Fig. 2: the susceptibility is positive and rises logarithmically at high temperatures, whereas there appears to be a weak diamagnetic region at low T. The transition point is located slightly below T_c, at $T \approx 110$ MeV. The agreement with the free-case model even holds on the quantitative level, as the right panel of Fig. 5 shows, where the continuum estimate of Ref. [10] is compared to the hadron resonance gas model (dominated by the pionic contribution of Eq. (2.5)) at low T and to perturbation theory at high T (given by the quark contribution of Eq. (2.5)). The perturbative curves are obtained by taking into account QCD corrections in β_1^{f} to various orders. Thus, the lattice results confirm the prediction that the high-T behavior of χ_r is dictated by the QED β-function. This perturbative regime is observed to set in at considerably lower temperatures ($T \approx 200 - 300$ MeV) as one is used to for other QCD observables.
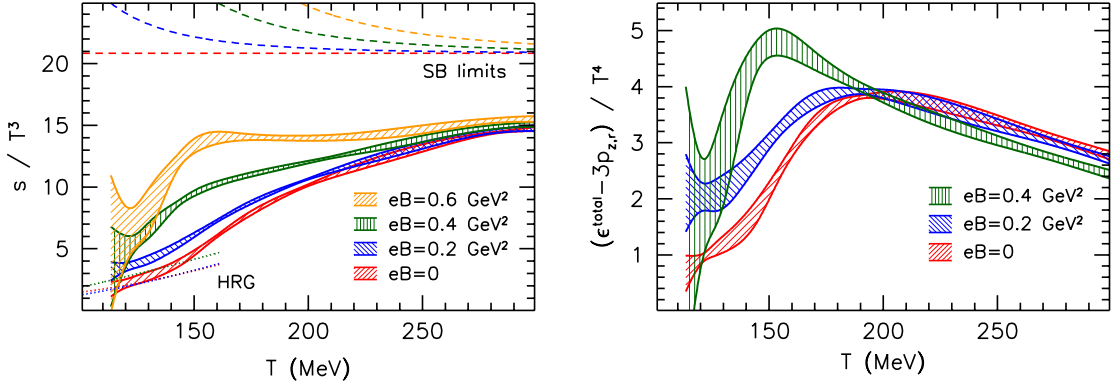

Figure 5: Left panel: the magnetic susceptibility of QCD as a function of the temperature. Results with different lattice approaches are collected. Right panel: comparison to the hadron resonance gas model and to perturbation theory, truncated at various orders of the strong coupling. Figures taken from Ref. [10].
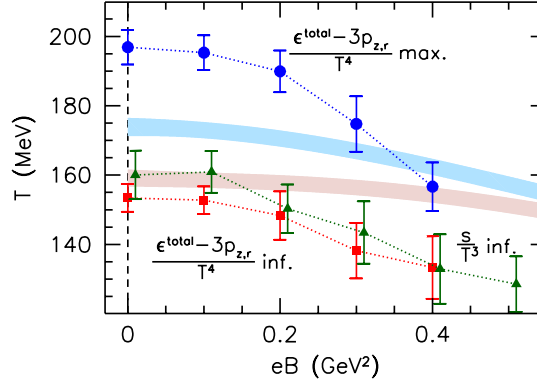
4. Equation of state for nonzero magnetic fields

Besides the susceptibility, the generalized integral method gives access to the complete B-dependence of the free energy density, and, through that, the full EoS, which has been determined in Ref. [10] for $0 < eB < 0.7$ GeV^2. In Fig. 6, I show the entropy density $s = -\partial f/\partial T$ and the interaction measure $\varepsilon^{\mathrm{total}} - 3p_\parallel$ (with a normalization by T^3 and by T^4, respectively). In the latter, $\varepsilon^{\mathrm{total}} = \varepsilon + \varepsilon^{\mathrm{field}}$ is the total energy density of the system, consisting of the matter energy $\varepsilon = -\partial f/\partial(1/T)$ and the field energy $\varepsilon^{\mathrm{field}} = eB \cdot \mathcal{M}$, see the discussion in Ref. [10].

The inflection point of both observables can be used to define T_c. This point is apparently shifted to lower temperatures as the magnetic field grows: the transition temperature is decreased by the magnetic field. The corresponding phase diagram is shown in Fig. 7. In the plot the maximum of the interaction measure is also indicated – this is not a measure for T_c but merely another

Figure 6: The entropy density (left panel) and the interaction measure (right panel) as functions of the temperature for various values of the background magnetic field. Figures taken from Ref. [10].

characteristic point marking the transition region. The results are also compared to the earlier determinations using the light quark condensate and the strange quark number susceptibility in Ref. [2], taken from the left panel of Fig. 1. All observables consistently show that $T_c(B)$ decreases.

Figure 7: The QCD phase diagram in the magnetic field – temperature plane with various definitions of T_c [10]. The purple band corresponds to the definition emplying the inflection point of the average light quark condensate and the blue band to that of the strange quark number susceptibility [2].

5. Implications

An intriguing question is what kind of implications the *B*-dependence of QCD thermodynamics may have for phenomenology. Several recent studies were devoted to address this question; in particular, in relation with heavy-ion collision experiments. In a peripheral collision intense magnetic fields are created that are the strongest at the center and fall off towards the edges of collision region – see, e.g. Ref. [20]. The gradient of the magnetic field induces a force density proportional to $\chi_r \nabla B^2$ that leads to an anisotropic 'squeezing' of the quark-gluon plasma. This effect was proposed in Ref. [14], where a simple estimate for the strength of the squeezing forces was also made. Whether the effect has a significant impact on, for example, the elliptic flow of the plasma, depends most predominantly on the lifetime of the generated magnetic fields and the thermalization of the expanding plasma. This is still the subject of intense debate and ongoing work.

Another quantity that might be of relevance in the context of heavy-ion collision phenomenology, is the static quark-antiquark potential. Ref. [21] has demonstrated that the magnetic field

induces a sizeable anisotropy in the potential and, accordingly, in the string tension σ such that $\sigma_\perp > \sigma_\parallel$. Heavy quarks thus become more strongly bound in the direction perpendicular to the magnetic field, while a separation along B costs less and less energy as the magnetic field increases. This suggests a Landau level-type picture, where the radius of the orbits decreases with B. In Ref. [21] it was speculated that the parallel string tension might even vanish at some critical magnetic field. In addition, the possible relevance of the results for hadronization processes in heavy-ion collisions was also addressed, although the magnetic fields are unlikely to live that long.

Finally, various lattice studies were performed recently to discuss the chiral magnetic effect: the generation of an electric current (electric polarization) due to the interplay of the background magnetic field and topologically non-trivial domains in the quark-gluon plasma [22]. This effect was quantified on the lattice by studying current-current correlators, by coupling quarks to a chiral chemical potential, by studying the generated current on classical instanton configurations or by analyzing correlators of the electric dipole moment with chirality or with the topological charge density [23, 24]. In Ref. [24] we also compared the continuum extrapolated lattice results to a model based on the lowest Landau-level approximation and massless quarks (cf. Ref. [25]). This simple model was found to overestimate the correlation coefficient by almost an order of magnitude – revealing a substantial difference between quasi-free quarks used in model approaches and fully interacting quarks in realistic physical situations.

6. Summary

In this talk, I summarized a set of recent lattice results about QCD in background magnetic fields. In particular, I discussed four different lattice approaches to determine the leading dependence of the equation of state on the magnetic field – characterized by the QCD magnetic susceptibility χ_r. All four methods give fully consistent results, showing that the thermal QCD medium is strongly paramagnetic at high temperatures. In addition, the results also indicate the presence of a weakly diamagnetic region at low T. I argued that this behavior can be explained in terms of a simple free-case model, see Fig. 2. Namely, the low-temperature diamagnetism stems from charged pions, while the high-T paramagnetism from quasi-free charged quarks. The model agrees with the lattice results even quantitatively, see the comparison in the right panel of Fig. 5.

In the second part of the talk I discussed the QCD equation of state in the presence of background magnetic fields. In this case, the concept of the pressure must be generalized – to unambiguously define the pressure in the direction perpendicular to B one must distinguish between the B- and Φ-schemes, see the discussion in Sec. 3. In the Φ-scheme the pressures develop an anisotropy that becomes sizeable as the magnetic field grows. In addition to the pressures, various observables including the entropy density and the interaction measure have been determined recently, see Fig. 6. Characteristic points of these observables can be used to define T_c – the so obtained phase diagram is consistent with earlier determinations and exhibits a *decreasing $T_c(B)$* transition line.

Some of the magnetic field-induced effects may also have relevance for heavy-ion phenomenology. The last part of the talk was devoted to briefly summarize these research directions. A better understanding of the time- and space-dependence of the magnetic field in the early stages of the collisions is necessary for controlled predictions.

References

[1] D. Kharzeev, K. Landsteiner, A. Schmitt, and H.-U. Yee *Lect.Notes Phys.* **871** (2013) 1–624.

[2] G. Bali, F. Bruckmann, G. Endrődi, Z. Fodor, et al. *JHEP* **2012** (2012) 1, [arXiv:1111.4956].

[3] M. D'Elia, S. Mukherjee, and F. Sanfilippo *Phys. Rev. D* **82** (2010) 051501, [arXiv:1005.5365]; V. Bornyakov, P. Buividovich, et al. *Phys.Rev.* **D90** (2014) 034501, [arXiv:1312.5628]; E. M. Ilgenfritz, M. Müller-Preussker, et al. *Phys.Rev.* **D89** (2014) 054512, [arXiv:1310.7876].

[4] A. J. Mizher et al. *Phys. Rev. D* **82** (2010) 105016, [arXiv:1004.2712].

[5] G. Bali et al. *Phys.Rev.* **D86** (2012) 071502, [arXiv:1206.4205]; F. Bruckmann, G. Endrődi, and T. G. Kovács *JHEP* **1304** (2013) 112, [arXiv:1303.3972].

[6] J. O. Andersen, W. R. Naylor, and A. Tranberg arXiv:1411.7176.

[7] G. Bali et al. *Nucl.Phys.* **A931** (2014) 752–757; G. Endrődi arXiv:1410.8028.

[8] K. Szabó *PoS* **LATTICE2013** (2014) 014, [arXiv:1401.4192]; M. D'Elia arXiv:1502.0604.

[9] J. S. Schwinger *Phys.Rev.* **82** (1951) 664–679; G. V. Dunne hep-th/0406216.

[10] G. Bali, F. Bruckmann, G. Endrődi, et al. *JHEP* **1408** (2014) 177, [arXiv:1406.0269].

[11] G. 't Hooft *Nucl. Phys.* **B153** (1979) 141.

[12] G. Bali, F. Bruckmann, G. Endrődi, F. Gruber, et al. *JHEP* **1304** (2013) 130, [arXiv:1303.1328].

[13] G. Bali, F. Bruckmann, G. Endrődi, et al. *PoS* **LATTICE2013** (2013) 182, [arXiv:1310.8145].

[14] G. Bali, F. Bruckmann, G. Endrődi, et al. *Phys.Rev.Lett.* **112** (2014) 042301, [arXiv:1311.2559].

[15] L. Levkova and C. DeTar *Phys.Rev.Lett.* **112** (2014), no. 1 012002, [arXiv:1309.1142].

[16] G. Endrődi *Phys.Rev.* **D90** (2014), no. 9 094501, [arXiv:1407.1216].

[17] C. Bonati, M. D'Elia, M. Mariti, et al. *Phys.Rev.Lett.* **111** (2013) 182001, [arXiv:1307.8063].

[18] C. Bonati, M. D'Elia, M. Mariti, et al. *Phys.Rev.* **D89** (2014), no. 5 054506, [arXiv:1310.8656].

[19] Y. Aoki, Z. Fodor, S. D. Katz, and K. K. Szabó *JHEP* **01** (2006) 089, [hep-lat/0510084].

[20] W.-T. Deng and X.-G. Huang *Phys.Rev.* **C85** (2012) 044907, [arXiv:1201.5108].

[21] C. Bonati, M. D'Elia, M. Mariti, et al. *Phys.Rev.* **D89** (2014), no. 11 114502, [arXiv:1403.6094].

[22] D. E. Kharzeev et al. *Nucl.Phys.* **A803** (2008) 227–253, [arXiv:0711.0950].

[23] P. Buividovich et al. *Phys.Rev.* **D80** (2009) 054503, [arXiv:0907.0494]; A. Yamamoto *Phys.Rev.Lett.* **107** (2011) 031601, [arXiv:1105.0385]; P. Buividovich *Nucl.Phys.* **A925** (2014) 218–253, [arXiv:1312.1843]; M. Abramczyk et al. *PoS* **LAT2009** (2009) 181, [arXiv:0911.1348]; P. Buividovich et al. *Phys.Rev.* **D81** (2010) 036007, [arXiv:0909.2350].

[24] G. Bali, F. Bruckmann, G. Endrődi, Z. Fodor, et al. *JHEP* **1404** (2014) 129, [arXiv:1401.4141].

[25] G. Basar, G. V. Dunne, and D. E. Kharzeev *Phys.Rev.* **D85** (2012) 045026, [arXiv:1112.0532].